Revision 3

Apexite, $NaMg(PO_4)\cdot 9H_2O$, a new struvite-type phase with a heteropolyhedral cluster.

ANTHONY R. KAMPF[1]*, STUART J. MILLS[2], BARBARA P. NASH[3], MARTIN JENSEN[4], AND TONY NIKISCHER[5]

[1]Mineral Sciences Department, Natural History Museum of Los Angeles County, 900 Exposition Boulevard, Los Angeles, CA 90007, USA
[2]Geosciences, Museum Victoria, GPO Box 666, Melbourne 3001, Victoria, Australia
[3]Department of Geology and Geophysics, University of Utah, Salt Lake City, UT 84112, USA
[4]8720 Rainbow Trout Court, Reno, NV 89523, USA
[5]1885 Seminole Trail, Charlottesville, VA 22901, USA
*Email: akampf@nhm.org

Abstract

Apexite (IMA2015-002), $NaMg(PO_4)\cdot 9H_2O$, is a new mineral from the Apex mine, Lander County, Nevada, USA, where it occurs as a low-temperature secondary mineral on massive quartz matrix in association with andersonite, calcite, čejkaite, gaylussite, and goethite. Apexite forms colorless needles up to 0.5 mm in length. The streak is white. Crystals are transparent and have vitreous to satiny luster. The Mohs hardness is about 2, the tenacity is brittle, the fracture is curved, and crystals exhibit one perfect cleavage on {100}. The measured density is 1.74(1) g/cm^3 and the calculated density is 1.741 g/cm^3. Electron microprobe analyses provided: Na_2O

9.26, MgO 14.42, P_2O_5 23.31, H_2O 53.01 (structure), total 100.00 wt% (normalized). The empirical formula (based on 13 O *apfu*) is: $Na_{0.91}Mg_{1.09}P_{1.00}O_{13.00}H_{17.91}$. Apexite is triclinic, *P*-1, $a = 6.9296(7)$, $b = 11.9767(13)$, $c = 14.9436(19)$ Å, $\alpha = 92.109(6)$, $\beta = 102.884(7)$, $\gamma = 105.171(7)°$, $V = 1160.9(2)$ Å^3, and $Z = 4$. The eight strongest lines in the X-ray powder diffraction pattern are [d_{obs} in Å(*I*)(*hkl*)]: 14.63(35)(001); 5.11(61)(021,-1-11,110,-120); 4.68(75)(0-22,-1-12,1-21,0-13); 4.301(96)(102,013,022,-113); 4.008(44)(-1-13,1-22); 2.876(46)(040); 2.762(100)(-2-13,2-31,0-34,-204,015); and 2.507(30)(212,025,-2-23). Apexite is a new struvite-type phase with a unique structure ($R_1 = 4.44\%$ for 1401 $F_o > 4\sigma F$) consisting of four components: (1) a $[Na_2Mg_4(H_2O)_{14}]^{10+}$ heteropolyhedral cation cluster; (2) a *trans* edge-sharing chain of $Na(H_2O)_6$ octahedra; (3) an isolated PO_4 group; and (4) an isolated H_2O group. The structural components are linked to one another only *via* hydrogen bonds. Its structure is related to that of hazenite.

Keywords: apexite; new mineral; crystal structure; struvite-type; heteropolyhedral cluster; hazenite; Apex mine, Nevada.

Introduction

The process by which minerals form efflorescent crusts on the walls of mine tunnels is generally similar to that by which minerals are deposited in saline lakes and playas. In both cases, minerals form as the result of the evaporation of ion-rich water, typically under oxidizing conditions and at ambient temperatures. The minerals formed are dependent on a variety of factors, but most importantly on the ion content and pH of the solution. Not surprisingly, some of the same minerals form in these topographically different environments, e.g. blödite, epsomite,

gaylussite, glauberite, etc. One important difference between mineral formation in mine tunnels and that in saline lakes is that organisms, specifically bacteria, are more likely to play a role in the latter rather than the former. The new mineral described herein was found as an efflorescent product on a tunnel wall in a uranium mine. Although associated with secondary uranium mineralization, it is a hydrated Na-Mg phosphate, and might be expected to occur, as well, in evaporative saline lake deposits and perhaps as the product of a biologically related process, such as is the case for the recently described mineral hazenite, $KNaMg_2(PO_4)_2 \cdot 14H_2O$ (Yang *et al*., 2011).

The new mineral is named apexite, for the locality, the Apex mine. The new mineral and name have been approved by the Commission on New Minerals, Nomenclature, and Classification of the International Mineralogical Association (IMA2015-002). The description is based on three cotype specimens. Two cotypes are deposited in the collections of the Natural History Museum of Los Angeles County, 900 Exposition Boulevard, Los Angeles, CA 90007, USA, catalogue numbers 65563 and 65564. One cotype specimen is housed in the collections of the Museum Victoria, Melbourne, Victoria, Australia, catalogue number M53381.

Occurrence and paragenesis

Apexite was found by one of the authors (MJ) at the Apex mine, about 4.5 km SSW of Austin, Lander Co., Nevada, USA (39°27’30”N 117°05’56”W). Much of the foregoing is taken from Jensen and Herrmann (2012). Historically, the Apex mine has been the largest producer of uranium in the state of Nevada. The deposit was discovered in 1953 and was originally named the Rundberg mine. The name was changed to Apex in 1955. The mine was most productive during the uranium boom of the mid 1950s and was active until 1966. Since then, several

different companies have conducted exploratory drilling, most recently in 2010, but there has been no additional mining. The extensive workings are all underground and consist of several adits; currently, access to all workings is blocked by iron gratings or backfill.

The deposit occurs within brecciated zones of leucocratic dikes at the contact between a Jurassic-age quartz monzonite intrusion and metamorphosed shales and quartzites of Cambrian age. The source of the uranium is thought to be Tertiary volcanism, which produced the leucocratic dikes. Sulfides (mostly pyrite) and carbonaceous matter in the metasediments provided the reducing conditions that caused the precipitation of the primary uranium minerals uraninite and coffinite from the uranium-enriched fluids. Phosphorous to form abundant secondary uranyl phosphates probably derived from the shales/phyllites.

Oxidative weathering of the deposit by meteoric water in recent times has yielded an extensive array of secondary uranyl phosphates, sulfates and carbonates, along with a variety of associated minerals. Apexite is a rare mineral in the secondary assemblage, formed as an efflorescence on mine walls. It occurs on massive quartz matrix in association with andersonite, calcite, čejkaite, gaylussite, and goethite. Crystals of apexite commonly contain inclusions of čejkaite. Čejkaite is known to form at relatively high pH – between 6.5 and 11.5 (Ondruš *et al*., 2003) – and it can be surmised that apexite also formed at high pH. Other minerals reported in the secondary assemblage include aragonite, autunite, baryte, chabazite-Ca, epsomite, graphite, gypsum, hydroglauberite, jarosite, magnesiozippeite, meta-autunite, metatorbernite, metauranocircite, natrozippeite, opal, pyrolusite, rutherfordine, sulfur, torbernite, uranocircite, uranopilite, and zippeite.

Physical and optical properties

Apexite occurs as colorless needles and blades up to 0.5 mm long in subparallel intergrowths (Fig. 1). Crystals are elongated on [100] and flattened on {001}, and exhibit the crystal forms {100}, {001}, {1-10}, {011}, and {0-12} (Fig. 2). Observations under crossed polars suggest that crystals commonly exhibit polysynthetic twinning on {010}; however, XRD study of apparently twinned crystals did not reveal a rational twin law. The mineral has white streak. Crystals are transparent and have vitreous to satiny luster. Apexite does not fluoresce in long or short wave ultraviolet light. The Mohs hardness is about 2, the tenacity is brittle, the fracture is curved, and crystals exhibit one perfect cleavage on {100}. The density measured by floatation in a mixture of methylene iodide and toluene is 1.74(1) g/cm^3. The calculated density based on the empirical formula and the unit cell refined from the single-crystal data is 1.741 g/cm^3. Apexite is slowly (minutes) soluble in water at room temperature and rapidly soluble in dilute HCl.

The mineral is biaxial, but because the $2V$ is close to 90°, the optic sign cannot be stated with certainty. The indices of refraction measured in white light are α = 1.475(1), β = 1.481(1), and γ = 1.487(1). The $2V_x$ determined using extinction data with EXCALIBR (Gunter *et al*., 2004) is 88.5(3) °; the calculated $2V$ is 90°. No dispersion or pleochroism was observed. The partially determined optical orientation is Z ^ **a** = 40°. The Gladstone-Dale compatibility, 1 – (K_p/K_c) is –0.026 (excellent) based on the empirical formula and –0.025 (excellent) based on the ideal formula. (Mandarino 1981).

Chemical composition

Chemical analyses (6) were performed at the University of Utah using a Cameca SX-50 electron microprobe with four wavelength-dispersive spectrometers and utilizing Probe for EPMA software. Analytical conditions were 15 kV accelerating voltage, 10 nA beam current, a beam diameter of 10 μm, and counting times of 15 seconds. In the analytical routine, Na, Mg, and P were counted simultaneously, *i.e.*, first on their respective spectrometers. There was a small but measurable loss of Na under the electron beam that was monitored during each spot analysis, and the Na intensity was calculated by extrapolating back to a zero time value. No other elements were detected by EDS. Raw X-ray intensities were corrected for matrix effects with a $\phi(\rho z)$ algorithm (Pouchou and Pichoir, 1991). There was minimal beam damage; however, as is typical of highly hydrated phases with weakly held H_2O (in this instance, over 50% by weight), apexite partially dehydrates under vacuum either during carbon coating or in the microprobe chamber. This H_2O loss results in higher concentrations for the remaining constituents than are to be expected for the fully hydrated phase. Because insufficient material is available for a direct determination of H_2O, it has been calculated based upon the structure determination. The analyzed constituents have then been normalized to provide a total of 100% when combined with the calculated H_2O. Analytical data are given in Table 1.

The empirical formula (based on 13 O apfu) is $Na_{0.91}Mg_{1.09}P_{1.00}O_{13.00}H_{17.91}$. The ideal formula is $NaMg(PO_4)\cdot 9H_2O$, which requires Na_2O 10.18, MgO 13.24, P_2O_5 23.32, and H_2O 53.26, total 100.00 wt%.

It is perhaps worth noting that amount of H_2O loss noted above provides analytical results approximately fitting the 7-hydrate, $NaMg(PO_4)\cdot 7H_2O$, whose structure was reported by Mathew *et al*. (1982). While it may be tempting to conjecture that apexite converts to the 7-hydrate upon

136 H_2O loss, this is very unlikely to be the case because such a transformation would require a very
137 significant rearrangement of the structural components (see the discussion of the structure
138 below).
139
140 **X-ray crystallography and structure refinement**
141 Both powder and single-crystal X-ray studies were carried out using a Rigaku R-Axis
142 Rapid II curved imaging plate microdiffractometer, with monochromatized Mo*Kα* radiation. For
143 the powder-diffraction study, a Gandolfi-like motion on the φ and ω axes was used to randomize
144 the sample and observed *d*-spacings and intensities were derived by profile fitting using JADE
145 2010 software (Materials Data, Inc.). The powder data are presented in Table 2. Note that čejkaite
146 inclusions are common in apexite crystals and even a small amount of čejkaite leads to additional
147 peaks in the PXRD because čejkaite diffracts much more strongly than apexite. While care was
148 taken in selecting apexite crystals for PXRD, some contamination was unavoidable. Unit-cell
149 parameters refined from the powder data using JADE 2010 with whole pattern fitting are: a =
150 6.918(6), b = 11.990(6), c = 14.976(5) Å, α = 91.75(2), β = 102.71(3), γ = 105.36(3)°, and V =
151 1163.3(12) Å^3.
152 The Rigaku CrystalClear software package was used for processing structure data,
153 including the application of an empirical multi-scan absorption correction using ABSCOR
154 (Higashi, 2001). The structure was solved by direct methods using SIR2004 (Burla *et al.*, 2005).
155 SHELXL-2013 (Sheldrick, 2008) was used for the refinement of the structure. Difference Fourier
156 syntheses located all H atom positions, which were then refined with soft restraints of 0.90(3) Å
157 on the O–H distances and 1.42(3) Å on the H–H distances and with the U_{eq} of each H set to 1.5
158 times that of the donor O atom. A very thin needle was used for the data collection because

polysynthetic twinning is pervasive in thicker prisms. The small size and weak diffracting ability of the crystal provided a relatively small data set and a less than optimal data-to-parameter ratio. Data collection and refinement details are given in Table 3, atom coordinates and displacement parameters in Table 4, polyhedral bond distances in Table 5, hydrogen-bond distances, angles, and BV contributions in Table 6, and a bond valence analysis in Table 7.

Discussion

The structure of apexite (Fig. 3) contains four structural components: (1) a $[Na_2Mg_4(H_2O)_{14}]^{10+}$ heteropolyhedral cation cluster (Fig. 4); (2) a *trans* edge-sharing chain of $Na(H_2O)_6$ octahedra along [100]; (3) an isolated PO_4 group; and (4) an isolated H_2O group. The cation cluster has an edge-sharing dimer of $Na(H_2O)_6$ trigonal prisms at its center and is decorated with four $Mg(H_2O)_6$ octahedra that share edges with the $Na(H_2O)_6$ trigonal prisms. The structural components are linked to one another only *via* hydrogen bonds.

Minerals with structures containing isolated PO_4 or AsO_4 groups are quite rare. They are limited to the arsenates rösslerite, $Mg(AsO_3OH)\cdot 7H_2O$, and joteite, $Ca_2CuAl[AsO_4][AsO_3(OH)]_2(OH)_2\cdot 5H_2O$, and the phosphates phosphorrösslerite, $Mg(PO_3OH)\cdot 7H_2O$, struvite, $NH_4Mg(PO_4)\cdot 6H_2O$, struvite-(K), $KMg(PO_4)\cdot 6H_2O$, and hazenite, $KNaMg_2(PO_4)_2\cdot 14H_2O$. Struvite, struvite-(K), hazenite, and similar synthetic compounds are referred to as struvite-type phases (see Yang *et al*., 2011, and references therein). "Struvite-type" in this context does not imply isostructural compounds; rather it indicates phases whose structures exhibit a number of similar features: (1) the general chemical formula is $M^+X^{2+}(YO_4)\cdot nH_2O$, where M is a large cation, X is a medium-sized octahedrally coordinated cation, Y is P or As, and n = 6 to 8; (2) the M and X cations are completely surrounded by H_2O

groups; (3) no H_2O groups are shared between $X(H_2O)_6$ octahedra; (4) the PO_4 or AsO_4 groups are unconnected and normal (non-acid); and (5) the structural components are held together by an extensive system of hydrogen bonds, including strong triple bonds between adjacent faces of $X(H_2O)_6$ octahedra and YO_4 tetrahedra.

Apexite has all of the features of a struvite-type phase noted above and clearly qualifies as such. It does have a higher H_2O content (n = 9) than has previously been noted for struvite-type phases; however, it also has an isolated H_2O group, which is atypical for these phases. Two of the other structural components in the apexite structure also are not found in any of the other struvite-type phases: the *trans* edge-sharing chains of $Na(H_2O)_6$ octahedra and the edge-sharing clusters of $Mg(H_2O)_6$ octahedra and $Na(H_2O)_6$ trigonal prisms. The structure of $NaMg(PO_4)\cdot 7H_2O$ (Mathew *et al*., 1982) does contain *trans* edge-sharing chains of octahedra, but $Na(H_2O)_6$ and $Mg(H_2O)_6$ octahedra alternate in those chains. The structure of hazenite (Yang *et al*., 2011) has $Na(H_2O)_6$ trigonal prisms that share edges with one another and with $Mg(H_2O)_6$ octahedra; however, in the hazenite structure, the trigonal prisms form edge-sharing chains that are decorated with Mg octahedra, while in the apexite structure, the trigonal prisms form dimers that are decorated with $Mg(H_2O)_6$ octahedra (Fig. 4).

Implications

Apexite is a new struvite-type phase with a number of interesting structural features not found in other known struvite-type phases. Struvite and other phosphates in this class of compounds are noted for commonly having biologically related modes of formation. There is no indication that the formation of apexite at the Apex mine was in any way biologically related; however, the general conditions of formation of apexite, i.e. ambient temperature and relatively

high pH, are consistent with those for other struvite-type phases, such as struvite and hazenite. Therefore, it seems plausible that apexite could be found elsewhere as a biologically formed phase. Considering the high level of interest in struvite and struvite-type phases in biological and environmental systems, the unique structural features found in apexite, and in particular its $[Na_2Mg_4(H_2O)_{14}]^{10+}$ cation cluster, deserve careful scrutiny. The conditions necessary for this cation cluster to exist in solution are worth investigating, as are the implications that this may have on systems in which struvite-type phases play a part.

Acknowledgements

Daniel Atencio and an anonymous reviewer are thanked for their constructive comments on the manuscript. Giovanni Ferraris is thanked for helpful comments on the twinning. This study was funded, in part, by the John Jago Trelawney Endowment to the Mineral Sciences Department of the Natural History Museum of Los Angeles County.

References

Brese, N.E. and O'Keeffe, M. (1991) Bond-valence parameters for solids. *Acta Crystallographica*, **B47**, 192–197.

Brown, I.D. and Altermatt, D. (1985) Bond-valence parameters from a systematic analysis of the inorganic crystal structure database. *Acta Crystallographica*, **B41**, 244–247.

Burla, M.C., Caliandro, R., Camalli, M., Carrozzini, B., Cascarano, G.L., De Caro, L., Giacovazzo, C., Polidori, G. and Spagna, R. (2005) SIR2004: an improved tool for crystal structure determination and refinement. *Journal of Applied Crystallography*, **38**, 381–388.

Gunter, M.E., Weaver, R., Bandli, B.R., Bloss, F.D., Evans, S.H., and Su, S.C. (2004) Results from a McCrone spindle stage short course, a new version of EXCALIBR, and how to build a spindle stage. *The Microscope*, **52**, 1, 23−39.

Higashi, T. (2001) *ABSCOR*. Rigaku Corporation, Tokyo.

Jensen, M. and Herrmann, J. (2012) Uranium mineralization at the Apex Mine, Lander County, Nevada. *Rocks and Minerals*, **87**, 270–276.

Mathew, M., Kingbury, P., Takagi, S. and Brown, W.E. (1982) A new struvite-type compound, magnesium sodium phosphate heptahydrate. Acta Crystallographica, **B38**, 40–44.

Ondruš, P., Skála, R., Veselovský, F. Sejkora, J., and Vitti, C. (2003) Čejkaite, the triclinic polymorph of $Na_4(UO_2)(CO_3)_3$ – a new mineral from Jáchymov, Czech Republic. *American Mineralogist*, **88**, 686–693.

Pouchou, J. L., & Pichoir, F. (1991). Quantitative analysis of homogeneous or stratified microvolumes applying the model "PAP". In: Heinrich, K.F.J. and Newbury, D.E. *Electron Probe Quantitation* (pp. 31-75). Plenum Press, N.Y.

Sheldrick, G.M. (2008) A short history of *SHELX*. *Acta Crystallographica*, **A64**, 112–122.

Wood, R.M. and Palenik, G.J. (1999) Bond valence sums in coordination chemistry. Sodium-oxygen complexes. *Inorganic Chemistry*, **38**, 3926–3930.

Yang, H. Sun, H.J. and Downs, R.T. (2011) Hazenite, $KNaMg_2(PO_4)_2{\cdot}14H_2O$, a new biologically related phosphate mineral, from Mono Lake, California, U.S.A. *American Mineralogist*, **96**, 675–681.

248 Table 1. Electron microprobe data for apexite.

Constituent	wt%	Range	SD	Standard	Normalized
Na_2O	10.42	8.02–13.36	1.74	albite	9.26
MgO	16.23	14.66–18.60	1.74	diopside	14.42
P_2O_5	26.24	23.88–30.65	2.87	apatite	23.31
H_2O*	53.01				53.01
Total	105.90				100.00

249 * Based on the structure with 13 O *apfu*.
250

Table 2. Powder X-ray diffraction data for apexite.

I_{obs}	d_{obs}	d_{calc}	I_{calc}	*hkl*
35	14.63	14.5436	48	0 0 1
		9.4712	3	0-1 1
		8.6370	3	0 1 1
16	7.25	7.2718	29	0 0 2
8	6.36	6.4279	15	0-1 2
20	5.84	5.9011	20	0 1 2
		5.7549	8	0 2 0
		5.5330	6	0-2 1
		5.4597	5	1 0 1
		5.3443	9	-1 1 2
61	5.11	5.1862	21	0 2 1
		5.1712	11	-1-1 1
		5.0757	5	1 1 0
		5.0596	8	-1 2 0
		4.9370	3	-1 2 1
		4.8479	6	0 0 3
75	4.68	4.7356	23	0-2 2
		4.6917	13	-1-1 2
		4.6348	12	1-2 1
		4.6268	10	0-1 3
		4.4860	7	1 1 1
		4.4466	4	1-1 2
		4.4155	8	-1 0 3
		4.3665	5	-1 2 2
96	4.301	4.3540	41	1 0 2
		4.3240	4	0 1 3
		4.3185	10	0 2 2
		4.2734	32	-1 1 3
44	4.008	3.9866	18	-1-1 3
		3.9684	21	1-2 2
		3.8814	10	-1-2 1
14	3.805	3.8089	4	1 2 0
		3.7976	14	-1 3 0
		3.7156	4	-1 3 1
		3.5651	5	0-1 4
		3.5338	7	0-3 2
12	3.423	3.4579	6	-2 1 1
		3.3766	6	0 1 4
		3.3352	7	1-2 3
17	3.265	3.2682	17	0 3 2
		3.1653	4	1 1 3
		3.1571	3	0-3 3
		3.1395	9	2-1 1
19	3.103	3.1063	24	-2 1 3
		3.0155	3	2 0 1
		3.0088	4	-1-3 1
		2.9525	3	-1 4 0
		2.9150	13	2 1 0
		2.8856	8	0-1 5
46	2.876	2.8774	46	0 4 0
		2.8404	5	-2 3 2
100	2.762	2.8091	24	-2-1 3
		2.7765	32	2-3 1
		2.7731	27	0-3 4
		2.7662	5	-2 0 4
		2.7588	29	0 1 5
		2.7361	4	2 1 1
		2.7298	8	2 0 2
		2.7253	3	1-4 2
27	2.673	2.7007	9	0-2 5
		2.6722	8	-2 2 4
5	2.584	2.5936	7	-2-1 4
		2.5856	4	-2-2 2
		2.5838	10	0-4 3
		2.5379	5	2 2 0
30	2.507	2.5084	29	2 1 2
		2.5025	3	0 2 5
		2.4928	4	-2-2 3
		2.4685	4	-2 4 2
13	2.435	2.4443	23	-2 3 4
		2.4279	5	-1-4 1
		2.3892	5	-1 5 0
		2.3678	8	0-4 4
		2.3612	4	-1 3 5
12	2.351	2.3568	7	-2-1 5
		2.2719	5	2 1 3
16	2.223	2.2361	3	-2-3 2
		2.2180	6	-2 3 5
		2.2077	3	-2 0 6
		2.1861	3	-2 5 0
		2.1832	4	-2 4 4
20	2.152	2.1770	3	2 0 4
		2.1720	3	-2-2 5
		2.1446	3	1-1 6
		2.1426	4	0-3 6
		2.1373	7	0 5 2
		2.1123	3	1 0 6
		1.9977	4	2-1 5
10	1.978	1.9842	4	2-4 4
		1.9722	4	-2 1 7
		1.9670	4	0 3 6
		1.9554	4	0 4 5
21	1.928	1.9423	3	3 1 1
		1.9252	7	2-3 5
		1.9204	5	-2-1 7
19	1.892	1.9077	3	-3 3 5
		1.9038	3	0-3 7
		1.8996	4	0-6 2
		1.8775	3	3-1 3
22	1.845	1.8475	5	-3 2 6
		1.8401	4	-1 1 8
		1.8331	5	-2-3 6
		1.8182	5	2-5 4
16	1.791	1.8105	3	3-5 1
		1.7925	3	3 2 1
		1.7891	7	2-2 6
13	1.779	1.7748	5	-2 0 8
		1.7731	7	0 4 6
		1.7701	6	0 1 8
		1.7576	5	2 4 2
19	1.723	1.7289	18	-4 2 2
		1.7274	3	0 5 5
		1.7152	5	-2 6 4
		1.6961	5	-2-5 1
10	1.672	1.6810	4	-3 6 2
		1.6758	4	0-6 5
		1.6594	5	-2 7 1

*Calculated lines with intensities less than 3 are not shown.

Table 3. Data collection and structure refinement details for apexite.

Diffractometer	Rigaku R-Axis Rapid II
X-ray radiation/power	Mo$K\alpha$ (λ = 0.71075 Å)/50 kV, 40 mA
Temperature	298(2) K
Chemical Formula	$NaMg(PO_4)\cdot 9H_2O$
Space group	*P*-1
Unit cell dimensions	a = 6.9296(7) Å
	b = 11.9767(13) Å
	c = 14.9436(19) Å
	α = 92.109(6)°.
	β = 102.884(7)°.
	γ = 105.171(7)°
V	1160.9(2) Å^3
Z	4
Density (for above formula)	1.742 g cm^{-3}
Absorption coefficient	0.388 mm^{-1}
F(000)	640
Crystal size	110 × 15 × 8 μm
θ range	3.11 to 19.94°
Index ranges	$-6 \le h \le 6$, $-11 \le k \le 11$, $-14 \le l \le 14$
Reflections collected/unique	8861/2113; R_{int} = 0.098
Reflections with $F > 4\sigma(F)$	1401
Completeness to θ = 19.94°	97.8%
Refinement method	Full-matrix least-squares on F^2
Parameters refined	397
GoF	1.075
Final R indices [$F > 4\sigma(F)$]	R_1 = 0.0444, wR_2 = 0.0813
R indices (all data)	R_1 = 0.0856, wR_2 = 0.1019
Largest diff. peak/hole	+0.46/–0.37 e A^{-3}

*$R_{int} = \Sigma|F_o^2 - F_o^2(\text{mean})|/\Sigma[F_o^2]$. GoF = $S = \{\Sigma[w(F_o^2 - F_c^2)^2]/(n-p)\}^{1/2}$. $R_1 = \Sigma||F_o| - |F_c||/\Sigma|F_o|$. $wR_2 = \{\Sigma[w(F_o^2 - F_c^2)^2]/\Sigma[w(F_o^2)^2]\}^{1/2}$; $w = 1/[\sigma^2(F_o^2) + (aP)^2 + bP]$ where a is 0.0263, b is 3.0425 and P is $[2F_c^2 + \text{Max}(F_o^2, 0)]/3$.

Table 4. Atom coordinates and displacement parameters (Å^2) for apexite.

	x/*a*	*y*/*b*	*z*/*c*	U_{eq}	U^{11}	U^{22}	U^{33}	U^{23}	U^{13}	U^{12}
Na1	0.7538(4)	0.0028(3)	0.9988(2)	0.0390(9)	0.0378(19)	0.036(2)	0.043(2)	0.0026(16)	0.0095(16)	0.0098(16)
Na2	0.9896(4)	0.4003(2)	0.5845(2)	0.0338(8)	0.0317(18)	0.0327(19)	0.037(2)	0.0005(15)	0.0070(15)	0.0114(15)
Mg1	0.8528(3)	0.1163(2)	0.60609(16)	0.0228(7)	0.0215(15)	0.0238(15)	0.0211(15)	0.0008(12)	0.0039(12)	0.0042(12)
Mg2	0.2012(4)	0.5829(2)	0.79178(16)	0.0245(7)	0.0235(15)	0.0247(16)	0.0262(16)	0.0051(13)	0.0079(12)	0.0061(13)
P1	0.7051(3)	0.73255(16)	0.66342(13)	0.0187(5)	0.0174(12)	0.0208(13)	0.0190(13)	0.0011(10)	0.0046(10)	0.0069(10)
P2	0.4859(3)	0.24050(17)	0.76778(13)	0.0209(6)	0.0174(13)	0.0214(13)	0.0224(14)	0.0010(10)	0.0036(10)	0.0038(10)
O1	0.5296(7)	0.7863(4)	0.6269(3)	0.0242(13)	0.023(3)	0.026(3)	0.028(3)	0.004(2)	0.005(2)	0.015(3)
O2	0.8935(7)	0.7856(4)	0.6244(3)	0.0264(13)	0.026(3)	0.027(3)	0.027(3)	0.003(2)	0.008(2)	0.008(3)
O3	0.6295(7)	0.5992(4)	0.6370(3)	0.0239(13)	0.030(3)	0.016(3)	0.024(3)	-0.004(2)	0.006(2)	0.005(2)
O4	0.7735(7)	0.7565(4)	0.7705(3)	0.0291(13)	0.030(3)	0.033(3)	0.024(3)	0.001(3)	0.006(3)	0.007(3)
O5	0.4329(7)	0.1076(4)	0.7640(3)	0.0272(13)	0.033(3)	0.021(3)	0.025(3)	-0.002(2)	0.007(3)	0.004(3)
O6	0.3481(7)	0.2850(4)	0.8197(3)	0.0315(14)	0.022(3)	0.036(3)	0.038(3)	-0.006(3)	0.008(3)	0.011(3)
O7	0.4493(7)	0.2787(4)	0.6695(3)	0.0313(14)	0.029(3)	0.039(3)	0.022(3)	0.009(3)	0.002(2)	0.005(3)
O8	0.7145(7)	0.2964(4)	0.8181(3)	0.0244(13)	0.019(3)	0.025(3)	0.028(3)	0.004(2)	0.004(2)	0.004(2)
OW9	0.9574(8)	0.2219(5)	0.7256(4)	0.0408(16)	0.023(3)	0.055(4)	0.038(4)	-0.025(3)	-0.001(3)	0.011(3)
H9A	0.085(5)	0.242(7)	0.761(4)	0.061						
H9B	0.877(8)	0.237(7)	0.761(4)	0.061						
OW10	0.7478(8)	0.0078(5)	0.4870(3)	0.0341(14)	0.024(3)	0.046(4)	0.029(4)	-0.017(3)	0.000(3)	0.012(3)
H10A	0.630(6)	0.001(6)	0.446(4)	0.051						
H10B	0.824(8)	-0.021(6)	0.455(4)	0.051						
OW11	0.6122(8)	0.0150(4)	0.6518(4)	0.0315(14)	0.036(3)	0.021(3)	0.042(4)	0.000(3)	0.020(3)	0.008(3)
H11A	0.584(11)	-0.061(3)	0.651(5)	0.047						
H11B	0.558(11)	0.042(5)	0.694(4)	0.047						
OW12	0.0462(7)	0.0141(4)	0.6550(4)	0.0317(14)	0.027(3)	0.017(3)	0.045(4)	0.004(3)	0.000(3)	0.001(3)
H12A	0.003(9)	-0.062(3)	0.652(5)	0.048						
H12B	0.165(7)	0.041(5)	0.692(4)	0.048						
OW13	0.0859(7)	0.2236(5)	0.5550(3)	0.0278(13)	0.022(3)	0.039(3)	0.021(3)	0.007(3)	0.007(3)	0.005(3)
H13A	0.097(9)	0.213(6)	0.498(2)	0.042						
H13B	0.211(6)	0.240(6)	0.592(3)	0.042						
OW14	0.6726(7)	0.2273(5)	0.5564(3)	0.0303(14)	0.029(3)	0.039(3)	0.025(3)	0.005(3)	0.004(3)	0.015(3)
H14A	0.601(9)	0.224(6)	0.499(2)	0.045						
H14B	0.594(9)	0.242(6)	0.593(3)	0.045						
OW15	0.2059(8)	0.7014(5)	0.6987(4)	0.0541(18)	0.038(4)	0.065(4)	0.082(5)	0.056(4)	0.035(4)	0.029(4)
H15A	0.312(8)	0.728(7)	0.674(5)	0.081						
H15B	0.102(8)	0.724(7)	0.667(5)	0.081						

OW16	0.2102(9)	0.4599(5)	0.8842(3)	0.0366(15)	0.051(4)	0.040(4)	0.026(3)	0.007(3)	0.013(3)	0.021(3)
H16A	0.272(11)	0.407(5)	0.877(4)	0.055						
H16B	0.206(12)	0.470(6)	0.942(3)	0.055						
OW17	0.9405(8)	0.3315(5)	0.1318(4)	0.0370(15)	0.036(4)	0.043(4)	0.030(4)	-0.007(3)	0.001(3)	0.015(3)
H17A	0.049(8)	0.312(6)	0.166(4)	0.055						
H17B	0.891(10)	0.280(5)	0.082(3)	0.055						
OW18	0.3172(7)	0.4855(4)	0.7095(3)	0.0261(13)	0.031(3)	0.017(3)	0.035(4)	0.012(3)	0.010(3)	0.014(3)
H18A	0.360(9)	0.422(4)	0.723(5)	0.039						
H18B	0.413(8)	0.525(5)	0.680(4)	0.039						
OW19	0.5036(9)	0.6650(5)	0.8634(4)	0.0466(16)	0.038(4)	0.053(4)	0.036(4)	-0.015(3)	0.012(3)	-0.008(3)
H19A	0.589(11)	0.671(6)	0.825(5)	0.070						
H19B	0.515(12)	0.740(3)	0.878(5)	0.070						
OW20	0.9006(7)	0.4837(4)	0.7212(3)	0.0275(13)	0.024(3)	0.035(4)	0.025(4)	0.012(3)	0.006(3)	0.010(3)
H20A	0.842(9)	0.435(5)	0.756(4)	0.041						
H20B	0.805(8)	0.514(5)	0.691(4)	0.041						
OW21	0.7199(8)	-0.1940(5)	0.0242(3)	0.0372(15)	0.038(4)	0.044(4)	0.032(4)	0.004(3)	0.010(3)	0.014(3)
H21A	0.841(7)	-0.209(7)	0.038(5)	0.056						
H21B	0.670(10)	-0.216(6)	0.073(4)	0.056						
OW22	0.8693(8)	0.2000(5)	0.9691(4)	0.0343(14)	0.039(3)	0.037(4)	0.027(4)	0.005(3)	0.001(3)	0.016(3)
H22A	0.842(9)	0.243(6)	0.923(4)	0.051						
H22B	0.000(5)	0.213(7)	0.987(5)	0.051						
OW23	0.5766(9)	0.0484(5)	0.1105(3)	0.0403(15)	0.048(4)	0.033(4)	0.037(4)	0.010(3)	0.008(3)	0.008(3)
H23A	0.640(11)	0.114(3)	0.148(4)	0.060						
H23B	0.562(12)	-0.007(4)	0.149(4)	0.060						
OW24	0.9268(9)	-0.0327(5)	0.8772(3)	0.0419(15)	0.049(4)	0.036(4)	0.033(4)	-0.008(3)	0.004(3)	0.005(3)
H24A	0.892(12)	-0.101(3)	0.842(4)	0.063						
H24B	0.922(12)	0.020(4)	0.836(4)	0.063						
OW25	0.7661(7)	0.5004(5)	0.5014(4)	0.0328(14)	0.029(3)	0.041(4)	0.029(4)	-0.006(3)	0.004(3)	0.014(3)
H25A	0.646(7)	0.468(6)	0.461(4)	0.049						
H25B	0.730(10)	0.540(6)	0.544(4)	0.049						
OW26	0.2575(8)	0.4981(5)	0.0730(4)	0.0399(15)	0.050(4)	0.032(4)	0.034(4)	0.001(3)	0.014(3)	0.003(3)
H26A	0.291(11)	0.570(3)	0.100(5)	0.060						
H26B	0.152(8)	0.457(5)	0.092(5)	0.060						

Table 5. Selected bond distances (Å) for apexite.

Na1–OW21	2.360(6)	Mg1–OW9	2.023(5)	P1–O1	1.527(5)
Na1–OW22	2.380(6)	Mg1–OW10	2.036(5)	P1–O2	1.543(5)
Na1–OW23	2.406(6)	Mg1–OW12	2.057(5)	P1–O3	1.550(5)
Na1–OW23	2.411(6)	Mg1–OW11	2.077(5)	P1–O4	1.557(5)
Na1–OW24	2.471(6)	Mg1–OW13	2.093(5)	<P1–O>	1.544
Na1–OW24	2.483(6)	Mg1–OW14	2.099(5)		
<Na1–O>	2.419	<Mg1–O>	2.064	P2–O5	1.533(5)
				P2–O6	1.539(5)
Na2–OW25	2.367(6)	Mg2–OW15	2.022(5)	P2–O7	1.542(5)
Na2–OW13	2.433(6)	Mg2–OW17	2.059(5)	P2–O8	1.549(5)
Na2–OW25	2.441(6)	Mg2–OW16	2.064(5)	<P2–O>	1.541
Na2–OW20	2.507(6)	Mg2–OW19	2.084(5)		
Na2–OW14	2.538(6)	Mg2–OW18	2.085(6)		
Na2–OW19	2.538(6)	Mg2–OW20	2.120(6)		
<Na2–O>	2.470	<Mg2–O>	2.073		

Table 6. Hydrogen bond distances (Å) and angles and related bond valence contributions for apexite.

Donor–H···Acceptor	D–H	H···A	D···A	<DHA	BV_D	BV_A
OW9–H9A···O6	0.89(3)	1.77(3)	2.652(7)	173(7)	0.78	0.22
OW9–H9B···O8	0.89(3)	1.82(3)	2.696(7)	167(8)	0.79	0.21
OW10–H10A···OW11	0.88(3)	1.93(3)	2.810(7)	174(6)	0.82	0.18
OW10–H10B···OW12	0.91(3)	2.04(5)	2.849(7)	148(6)	0.84	0.16
OW11–H11A···O1	0.88(3)	1.77(3)	2.642(7)	168(6)	0.77	0.23
OW11–H11B···O5	0.89(3)	1.78(3)	2.664(7)	171(7)	0.78	0.22
OW12–H12A···O2	0.88(3)	1.78(3)	2.644(7)	169(7)	0.78	0.22
OW12–H12B···O5	0.86(3)	1.87(3)	2.727(7)	174(7)	0.80	0.20
OW13–H13A···O2	0.88(3)	1.85(3)	2.716(7)	169(7)	0.80	0.20
OW13–H13B···O7	0.89(3)	1.73(3)	2.614(7)	176(6)	0.76	0.24
OW14–H14A···O1	0.88(3)	1.88(3)	2.762(7)	174(6)	0.81	0.19
OW14–H14B···O7	0.90(3)	1.79(3)	2.687(7)	177(7)	0.79	0.21
OW15–H15A···O1	0.89(3)	1.79(3)	2.679(7)	178(9)	0.79	0.21
OW15–H15B···O2	0.88(3)	1.79(3)	2.663(7)	169(9)	0.78	0.22
OW16–H16A···O6	0.87(3)	1.92(3)	2.745(7)	160(7)	0.80	0.20
OW16–H16B···OW26	0.88(3)	1.91(3)	2.773(7)	168(7)	0.81	0.19
OW17–H17A···O4	0.90(3)	1.78(4)	2.662(7)	168(7)	0.78	0.22
OW17–H17B···OW22	0.89(3)	1.87(4)	2.723(7)	160(7)	0.80	0.20
OW18–H18A···O6	0.90(3)	2.23(4)	2.988(7)	142(5)	0.39	0.11
OW18–H18A···O7	0.90(3)	2.16(5)	2.942(7)	146(6)	0.37	0.13
OW18–H18B···O3	0.91(3)	1.80(3)	2.706(6)	171(6)	0.80	0.20
OW19–H19A···O4	0.90(3)	1.78(5)	2.612(7)	151(6)	0.76	0.24
OW19–H19B					1.00	0
OW20–H20A···O8	0.88(3)	2.02(3)	2.888(6)	168(7)	0.85	0.15
OW20–H20B···O3	0.88(3)	1.86(3)	2.732(6)	171(7)	0.80	0.20
OW21–H21A···OW22	0.88(3)	2.01(3)	2.846(7)	157(6)	0.84	0.16
OW21–H21B···O6	0.90(3)	1.84(4)	2.694(7)	158(6)	0.79	0.21
OW22–H22A···O8	0.90(3)	1.84(3)	2.709(7)	163(6)	0.80	0.20
OW22–H22B					1.00	0
OW22–H23A					1.00	0
OW23–H23B···O5	0.90(3)	1.80(3)	2.695(7)	172(7)	0.79	0.21
OW24–H24A···O4	0.89(3)	1.87(3)	2.754(7)	170(8)	0.81	0.19
OW22–H22B					1.00	0
OW25–H25A···O3	0.89(3)	2.08(3)	2.965(7)	177(7)	0.88	0.12
OW25–H25B···O3	0.90(3)	1.88(3)	2.769(7)	170(7)	0.81	0.19
OW26–H26A···O8	0.88(3)	2.00(4)	2.839(7)	159(6)	0.82	0.18
OW26–H26B···OW17	0.88(3)	2.01(3)	2.876(8)	167(7)	0.85	0.15

Table 7. Bond valence analysis for apexite. Values are expressed in valence units.*

	O1	O2	O3	O4	O5	O6	O7	O8	OW9	OW10	OW11	OW12	OW13	OW14	OW15	OW16	OW17	OW18	OW19	OW20	OW21	OW22	OW23	OW24	OW25	OW26	Σ
Na1																					0.20	0.19	0.17 0.17	0.14 0.14			1.01
Na2													0.16	0.12				0.12		0.13					0.19 0.16		0.88
Mg1									0.41	0.40	0.37	0.35	0.34	0.33													2.21
Mg2															0.41	0.37	0.37	0.35	0.35	0.32							2.16
P1	1.23	1.18	1.16	1.14																							4.70
P2					1.21	1.19	1.18	1.16																			4.75
H9A						0.22			0.78																		1.00
H9B								0.21	0.79																		1.00
H10A										0.82	0.18																1.00
H10B										0.84		0.16															1.00
H11A	0.23										0.77																1.00
H11B					0.22						0.78																1.00
H12A		0.22										0.78															1.00
H12B					0.20							0.80															1.00
H13A		0.20											0.80														1.00
H13B							0.24						0.76														1.00
H14A	0.19													0.81													1.00
H14B							0.21							0.79													1.00
H15A	0.21														0.79												1.00
H15B		0.22													0.78												1.00
H16A						0.20										0.80											1.00
H16B																0.81										0.19	1.00
H17A				0.22													0.78										1.00
H17B																	0.80					0.20					1.00
H18A						0.11	0.13											0.76									1.00
H18B			0.20															0.80									1.00
H19A				0.24															0.76								1.00
H19B																			1.00								1.00
H20A								0.15												0.85							1.00
H20B			0.20																	0.80							1.00
H21A																					0.84	0.16					1.00
H21B						0.21															0.79						1.00
H22A								0.20														0.80					1.00
H22B																						1.00					1.00
H23A																							1.00				1.00
H23B					0.21																		0.79				1.00
H24A				0.19																				0.81			1.00
H24B																								1.00			1.00
H25A			0.12																						0.88		1.00
H25B			0.19																						0.81		1.00
H26A								0.18																		0.82	1.00
H26B																	0.15									0.85	1.00
Σ	1.86	1.82	1.87	1.79	1.84	1.93	1.76	1.90	1.98	2.06	2.10	2.09	2.06	2.05	1.98	1.98	2.10	2.03	2.11	2.10	1.83	2.35	2.13	2.09	2.04	1.86	

Mg^{2+}–O bond valence parameters from Brown and Altermatt (1985); P^{5+}–O from Brese and O'Keeffe (1991); Na^{+}–O from Wood and Palenik (1999); hydrogen-bond strengths based on O–O bond lengths from Brown and Altermatt (1985).Table 6. Bond-valence analysis for apexite. Values are expressed in valence units.

FIGURE CAPTIONS

Figure 1. Apexite blades with čejkaite (light yellow online) and colorless equant crystal of gaylussite (upper left); FOV 0.25 mm across.

Figure 2. Crystal drawing of apexite; clinographic projection in standard orientation.

Figure 3. The structure of apexite viewed slightly canted down [100], the $Na1(H_2O)_6$ chain direction. O–H bonds are shown as sticks and hydrogen bonds as thin lines. The unit is cell shown by red lines.

Figure 4. The $[Na_2Mg_4(H_2O)_{14}]^{10+}$ cation cluster in apexite (left) and the $[NaMg(H_2O)_8]_\infty$ chain in hazenite (right).

Figure 1

Figure 2

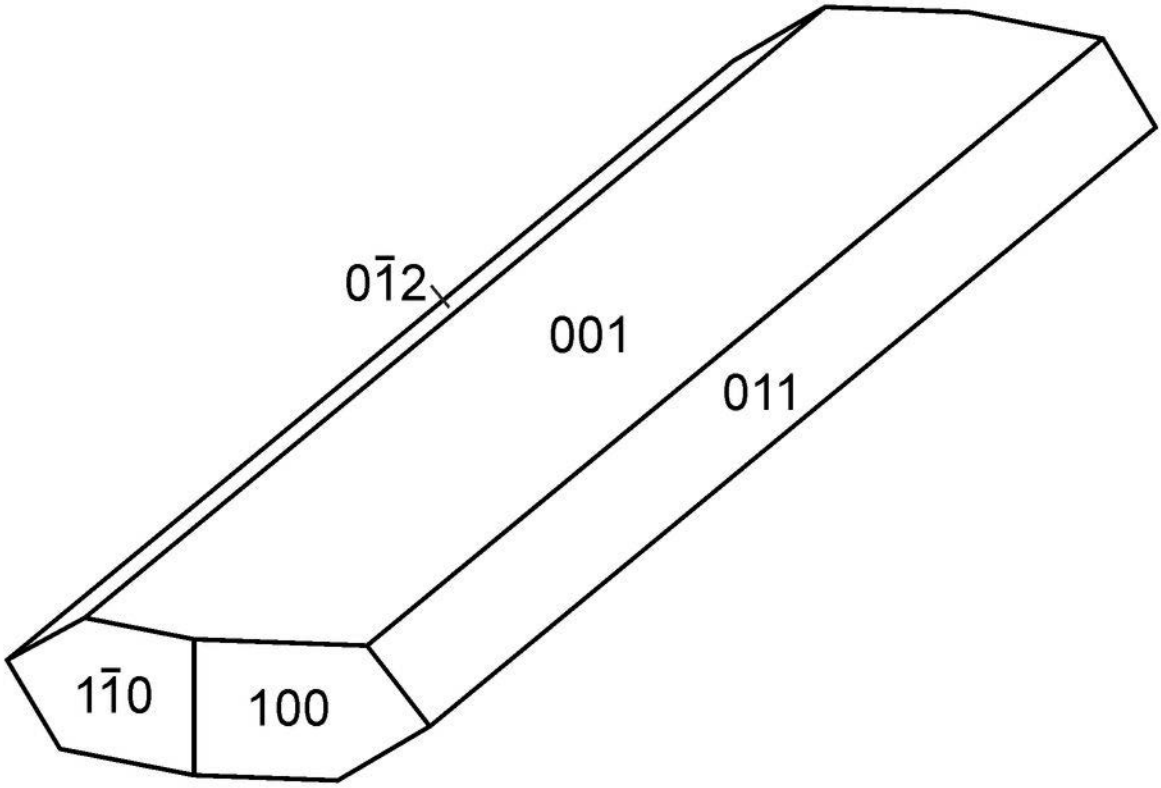

Figure 3

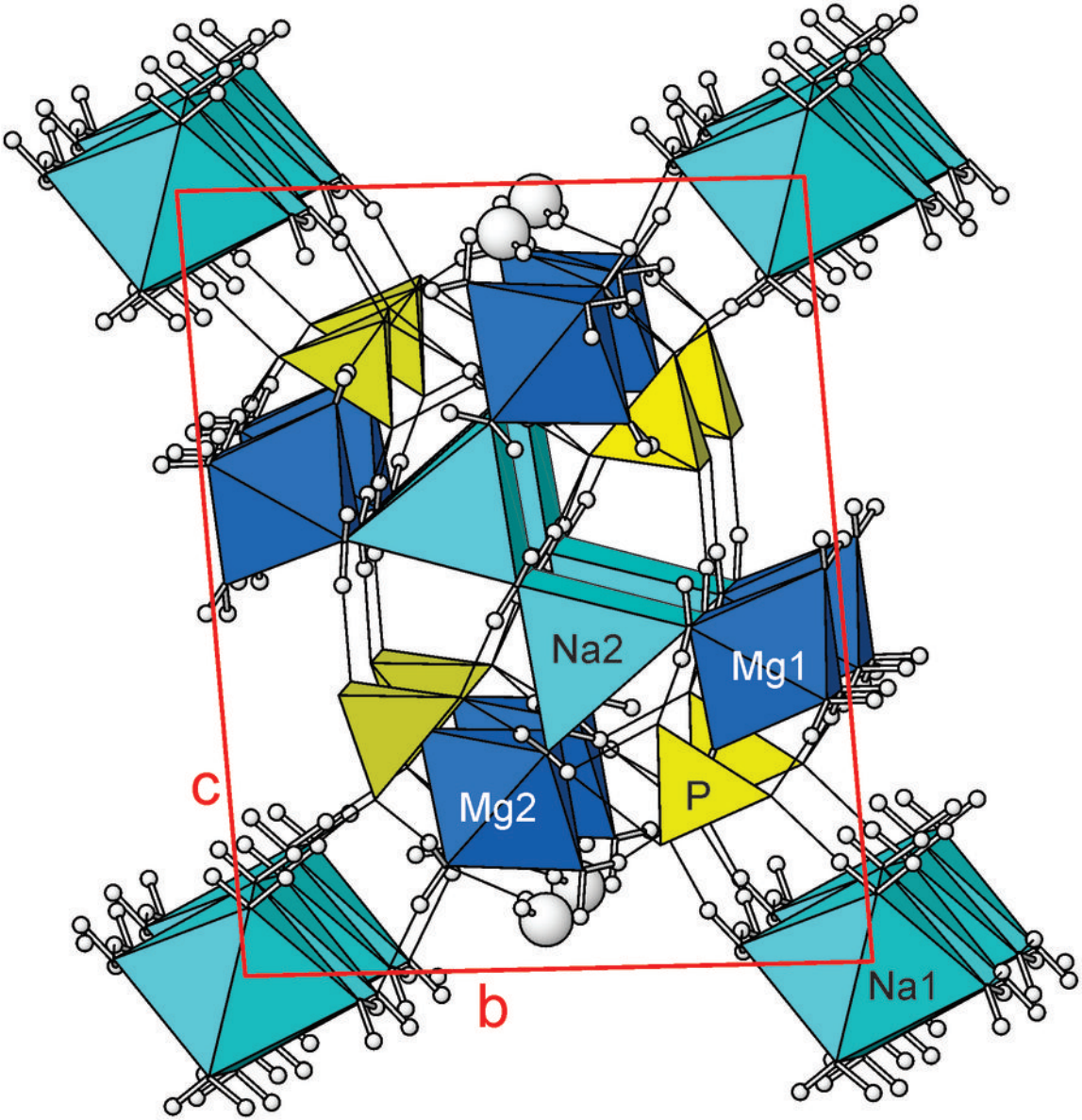

Figure 4